

EQST Modeling and Simulation of Surge Arresters

Y. Späck-Leigsnering¹, E. Gjonaj¹, H. De Gerssem¹, T. Weiland¹, M. Gießel², V. Hinrichsen²

¹Technische Universität Darmstadt, Institut für Theorie Elektromagnetischer Felder,
Schlossgartenstr. 8, 64289 Darmstadt, spaeck@temf.tu-darmstadt.de

²Technische Universität Darmstadt, Fachgebiet Hochspannungstechnik,
Landgraf-Georg-Str. 4, 64283 Darmstadt

A coupled electro-quasistatic-thermal (EQST) method for the simulation of surge arresters is developed. In order to cope with the extremely short time scales associated with the strongly nonlinear electrical characteristic of the metal-oxide (MO) varistor material, a multi-rate time integration technique is adopted. Besides, a model for the heat transfer in the arrester air gap is developed which takes into account radiation and natural convection by means of a nonlinear equivalent material. 2-Dimensional-Finite-Element-Method (2D-FEM) simulations for a large 550-kV-system station class arrester in continuous operation are carried out and validated against measurements. Furthermore, the method is used for the investigation of thermal stability under pulsed overvoltages as specified by the IEC operating duty test.

Index Terms—Power system protection, surge protection, arresters, thermal conductivity.

I. INTRODUCTION

Surge arresters are used to protect power system equipment from transient overvoltages caused by, e.g. lightning or switching events. A surge arrester consists basically of a vertical stack of varistor blocks made of MO material (generally zinc-oxide (ZnO)). The highly nonlinear I - V -characteristic of these varistors allows the arrester to clip voltage surges by absorbing large amounts of energy (cf. [1]).

The most serious limitation in the performance of surge arresters is posed by thermal stability. Electrical energy dissipation causes heating of the varistor blocks. As a result, the I - V -characteristic of the MO material is shifted towards higher electrical conductivities, thus, causing a further increase of heat losses. If not sufficiently compensated by heat transfer processes, this may lead to thermal runaway with major device failure [1]. In order to guarantee safe operation over the lifetime of arresters, the IEC 60099-4 standard specifies various operating duty tests [2]. The application of such tests on large, station class arresters under laboratory conditions, however, is extremely difficult [3]. This is why, the high-voltage engineering community is increasingly turning its attention towards numerical simulations as an alternative to conventional arrester design and testing [4].

In this paper, we propose a numerical method for surge arrester simulations. It includes a multi-rate time integration technique taking into account the different electrical and thermal time scales, respectively. Thermal radiation and convective heat transfer in the arrester air gap are modeled by means of an equivalent material with nonlinear thermal conductivity. This procedure is used in the investigation of thermal stability of a station class arrester according to IEC specifications.

II. SPECIMEN

The considered surge arrester is a 550-kV station class system available for testing purposes at the TU Darmstadt (see Fig. 1a). It contains a total of 76 vertically piled ZnO varistor

blocks as well as several metallic spacers and flanges amounting to a total stack height of 420 cm. This so called varistor column is enclosed within a porcelain housing (Fig. 1b). The most important figure for arrester operation is the electrical characteristic of its varistors. For the analyzed specimen, the electrical conductivity curves for different temperatures were obtained by single varistor measurements as depicted in Fig. 1c.

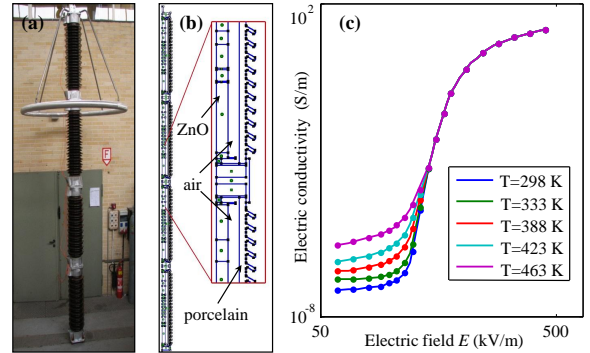


Fig. 1. (a) The 550-kV station class arrester equipped with a field grading ring. (b) Schematic view of the varistor column, air gap and porcelain housing. (c) Measured, temperature dependent electrical characteristics of the ZnO varistors.

III. NUMERICAL METHOD

A. EQST Simulation with Multi-Rate Time Stepping

The set of transient EQST equations is given by,

$$\partial_t \operatorname{div} \cdot (\varepsilon \operatorname{grad}(\phi)) + \operatorname{div} \cdot (\sigma \operatorname{grad}(\phi)) = 0, \quad (1)$$

$$\partial_t (c_v T) - \operatorname{div} \cdot (\lambda \operatorname{grad}(T)) = \dot{q}, \quad (2)$$

where ϕ is the electric potential and T the temperature. The electrical and thermal material properties are given by ε , σ , c_v and λ describing, permittivity, electrical conductivity, volumetric heat capacity and thermal conductivity, respectively. The two equations are coupled by the Joule loss power density, $\dot{q}(\mathbf{r}, t) = \sigma(\mathbf{r}, \mathbf{E}, T) \mathbf{E}^2 = \sigma(\mathbf{r}, \mathbf{E}, T) |\operatorname{grad} \phi|^2$.

A weak coupling approach is adopted. Equations (1), (2) are solved successively within every time step based on a standard 2D-FEM discretization of the surge arrester geometry. Hereby, the challenge is posed by the extremely different time scales characterizing electrical and thermal processes, respectively. The electrical conductivity at the working point varies by nearly 6 orders of magnitude within a single period of the AC voltage (cf. Fig. 1). The necessary time step for resolving these variations in (1) is estimated to $\Delta t_{el} < 10 \mu\text{s}$. On the other hand, thermal transients in the arrester develop over several hours. The minimum required thermal time step for the solution of (2) is $\Delta t_{th} \approx 1 \text{ min}$.

The basic idea of the multi-rate time integration scheme is illustrated in Fig. 2. The EQS problem (1) is advanced in time with Δt_{el} until a local electrical steady state is reached corresponding to a *time-periodic* variation of the arrester currents and voltages. Note that due to the nonlinearity of the problem, this state is very different from the usual time-harmonic solution arising in the linear case. Thus, a fully transient solution taking into account the nonlinear electrical conductivity of the ZnO varistors (Fig. 1) is necessary.

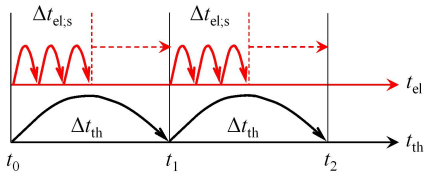


Fig. 2. Time stepping scheme with local EQS steady state.

The local electrical steady state is reached within a short interval of a few periods of the AC voltage with $\Delta t_{el,s} \ll \Delta t_{th}$. Assuming that the temperature distribution remains nearly constant, the total heat loss density within a thermal time step can be computed from the heat loss density per period at the local steady state. Thus, once an electrical steady state is reached, the heat conduction equation (2) can be advanced in time with the much larger time step, Δt_{th} . The resulting new temperature distribution is, then, used to compute a new local electrical steady state at the next time step.

B. Heat Transfer in the Air Gap

Thermal radiation and natural convection are of crucial importance as these two mechanisms determine the arrester resistance in continuous operation as well as its thermal stability under voltage surges. External thermal convection and radiation can be included in the simulation by applying appropriate boundary conditions. For the heat transfer in the air gap a nonlinear heat conduction model is applied. The air gap is assumed to be filled with an equivalent material with thermal conductivity

$$\lambda_{eq}(T) = \lambda_{air} + \lambda_{conv}(T) + \lambda_{rad}(T), \quad (3)$$

where λ_{eq} summarizes the combined effects of thermal conductivity, λ_{air} , natural convection, λ_{conv} , and radiation, λ_{rad} . The convective part is estimated separately for each arrester segment from the Nusselt number of a vertical annular cylinder

[5], depending on the inner and outer wall temperatures, geometric dimensions and fluid properties. The equivalent thermal conductivity describing thermal radiation is assumed to $\lambda_{rad}(T) = 4C_{12}T^3 r_1 \ln(r_2/r_1)$, where C_{12} is the radiation exchange factor and r_1 and r_2 are the inner and outer radii of the air gap, respectively. In the full paper, it will be shown that the heat flow rate provided by this model is identical with the one given by the Stefan-Boltzmann law for radiative heat transfer in the air gap.

IV. RESULTS

A. Arrester in Continuous Operation

Figure 3 (top) shows the stationary temperature distribution in the arrester (deposited on a grounded surface) after $\approx 4\text{h}$ of continuous operation at the rms-voltage $U_c = 345 \text{ kV}$ and power frequency $f = 50 \text{ Hz}$. In Fig. 3 (bottom), the transient temperature along the arrester axis is monitored every 8 minutes until stationary state is reached. The initial arrester and constant ambient air temperature is 293 K . Note that the temperature difference between the bottom and top segment of the arrester amounts to more than 80°C . Thus, the different arrester segments operate at very different working points on the electrical characteristics (Fig. 1). This result, as well as the temperature profiles obtained in the simulation, are in very good agreement with the measurement.

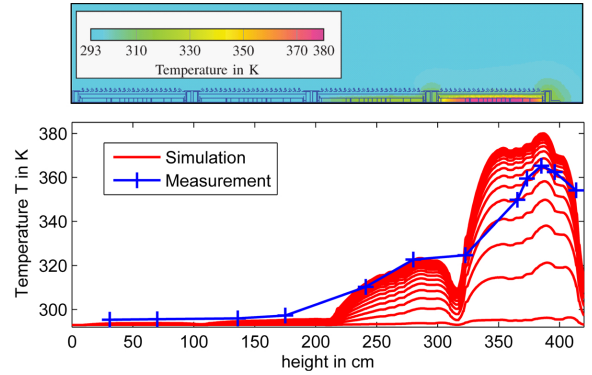


Fig. 3. Stationary temperature distribution in continuous operation (top). Temperature along arrester axis at different time instants; comparison with measurement (bottom).

In the full paper, EQST simulations for the investigation of thermal stability under pulsed overvoltages as specified by the IEC operating duty test [2] will be presented.

REFERENCES

- [1] V. Hinrichsen, *Metal-Oxide Surge Arresters in High-Voltage Power Systems - Fundamentals*, 3rd ed. Siemens AG, 2011.
- [2] IEC 60099-4, *Surge arresters - Part 4: Metal-oxide surge arresters without gaps for a.c. systems*, 2nd ed. Geneva, Switzerland: International Electrotechnical Commission (IEC), May 2009.
- [3] Z. Zheng, S. Boggs, T. Imai, and S. Nishiwaki, "Computation of arrester thermal stability," *IEEE Transactions on Power Delivery*, vol. 25, no. 3, pp. 1526–1529, Jul. 2010.
- [4] V. Hinrichsen, R. Göhler, M. Clemens, T. Steinmetz, and P. Riffon, "External grading systems for UHV metal-oxide surge arresters - a new approach to numerical simulation and dielectric testing," in *CIGRÉ Konferenz*, Mar. 2008.
- [5] VDI-Gesellschaft Verfahrenstechnik und Chemieingenieurwesen, Ed., *VDI Heat Atlas*. Springer, 2010.